Open Journal of Inorganic Chemistry, 2015, 5, 30-39
Published Online April 2015 in SciRes. http://www.scirp.org/journal/ojic
http://dx.doi.org/10.4236/ojic.2015.52005

Synthesis and Electrochemical Properties of Transparent Nanostructured $BaTiO_3$ Film Electrodes

Hongjun Wang*, Xinhua Cao, Fangke Liu, Shupei Guo, Xinxin Ren, Shuming Yang

College of Chemistry and Chemical Engineering, Xinyang Normal University, Xinyang, China
Email: *whj2016@163.com

Received 11 February 2015; accepted 10 April 2015; published 13 April 2015

Abstract

Transparent nanostructured $BaTiO_3$ film electrodes were synthesized on conductive substrates from $BaTiO_3$ nanocrystals forming at low temperature. Electrochemical and spectroelectrochemical methods were employed to investigate its properties of band energetics and the trap state at different pH values. The flat band edges greatly depended on the pH value of electrolyte, and the flat band edges were −0.70, −0.92 and −1.20 V vs saturated Ag/AgCl at the pH value of 3.0, 6.8 and 13.0, respectively. The results showed that trap state densities also highly depended on pH. The total trap state densities were 3.73×10^{15}, 4.02×10^{15} and 6.48×10^{16} cm^{-2} at pH value of 3.0, 6.8 and 13.0 respectively with maximum located at −0.36 V, −0.50 V and −0.80 V. The results obtained from CVs were in good agreement with that obtained from the measurements of time resolved currents. The size of the peak potentials in the cyclic voltammograms experiments was increased dramatically with the pH value increasing, indicating that traps were surface-related.

Keywords

Nanostructured $BaTiO_3$ Film, Electrochemistry, Spectroelectrochemistry, Band Energetics, Trap State

1. Introduction

Dye-sensitized solar cells (DSSCs) have attracted considerable attention in recent years due to their simple structure, low production cost and high performance [1]-[8]. The fundamental component of the DSSCs is the nanoporous electrode formed by nanocrystalline semiconductors. In order to improve the energy conversion ef-

*Corresponding author.

How to cite this paper: Wang, H.J., Cao, X.H., Liu, F.K., Guo, S.P., Ren, X.X. and Yang, S.M. (2015) Synthesis and Electrochemical Properties of Transparent Nanostructured $BaTiO_3$ Film Electrodes. *Open Journal of Inorganic Chemistry*, **5**, 30-39.
http://dx.doi.org/10.4236/ojic.2015.52005

ficiency, the development of new electrode materials seems to be one of the main research targets. In recent years, the metal oxides have been focused and employed typically such as wide band gap n-type semiconductors TiO_2, SnO_2, ZnO, *et al*. [9]-[12].

An obvious characteristic of nanoporous electrodes is the large density of surface states. They are the most important when the energies of these states lie in the band gap. Electrochemical and spectroelectrochemical methods are valuable in the study of their properties [11]-[18].

In comparison with these binary oxide semiconductors, the structure of oxide Barium titanate ($BaTiO_3$) was similar to anatase TiO_2, and could be loosely as a highly doped TiO_2 structure. The titanium atoms were 6-foldoctahedral coordination in Barium titanate ($BaTiO_3$). At the same time, the band gap of $BaTiO_3$ was nearly the same as that of anatase TiO_2 (3.2 ev) [19] [20]. But there is rarely report about nanostructured $BaTiO_3$ films so far.

In this study, monodispersed $BaTiO_3$ nanoparticles were prepared at low temperature and were fabricated as nanostructured $BaTiO_3$ films electrodes. The properties of band energetics and the trap state at different pH values were investigated with electrochemical and spectroelectrochemical techniques.

2. Experiment

2.1. Materials

$Ti(OCH(CH_3)_2)_4$, $Ba(OH)_2$ and Ethyl cellulose were purchased from Tianjin Chemical Company. $LiClO_4$, $HClO_4$, terpineol and tetramethylammonium hydroxide were purchased from Shanghai Nuotai Chemical Company. Optically transparent electrodes (OTE) were fabricated on an F-doped SnO_2-coated glass substrate. Water (R = 18.3 MΩ) was obtained from pure RF system. All the chemicals were reagent grade.

2.2. Preparation of Nanostructure $BaTiO_3$ Electrodes

Preparation of $BaTiO_3$ nanocrystals: $BaTiO_3$ nanocrystals were synthesized using a slightly modified previously published technique [21] [22]. At first, 5 mL of $Ti(n\text{-}OC_4H_9)_4$ and 1.5 mL of acetylacetone were mixed together. After addition of 10 mL of ethanol, the mixture solution was backflowed at 100˚C for 0.5 h. 4.7 g $Ba(OH)_2$ was dissolved in 60 mL of boiling water under vigorously stirring. After $Ba(OH)_2$ were completely dissolved, the former mixed solution was added to $Ba(OH)_2$ solution slowly under constantly at 100˚C in 1h. Then the mixture solution turned white and white crystals precipitate was formed. The precipitation was eventually washed with distilled water and dried at room temperature.

Preparation of nanostructured $BaTiO_3$ films: Resulting precipitate was washed with ethanol completely. 12.5 g of terpineol and 15 g of 10 wt% ethyl cellulose ethanol solution were added to the $BaTiO_3$ paste. Then the mixture was dispersed under sonication, and ethanol was removed by rotary-evaporator. The final solid were grounded with a mill.

$BaTiO_3$ sol was spread on the substrates by a glass rod with adhesive tapes as spacers. The films were dried at 105˚C and sintered at 500˚C for 30 min in air and finally cooled to room temperature.

3. Results and Discussions

3.1. Characterization of Nanostructured $BaTiO_3$ Film

X-ray diffraction (XRD) measurements were performed on a D 8 diffractometer (Bruker Co.) with Cu K_α (λ = 1.5405 Å) to identify the phase structure of samples. **Figure 1** shows the XRD patterns of the $BaTiO_3$ film which has a high pure cubic perovskite structure (JCPDS card 31-0174). The surface structure of the film could be obviously observed by SEM (S-4800, Hitachi, Japan) as shown in **Figure 2**. The SEM image reveal a bimodal particle distribution of the transparent films with small cubic particles with the diameter between 40 and 60 nm and large particles with the diameter 80 - 90 nm. The bimodal distribution is much desired in DSSCs which can increase light scattering and increase theoretical path length in the photoelectrode [13] [23].

The absorption spectra of the $BaTiO_3$ film deposited on a quartz substrate were recorded on an UV-1240 spectrophotometer (Shimadzu, Japan) as shown in **Figure 3**. Absorption tail at long wavelength was due to the diffusion and reflection of nanostructured $BaTiO_3$ film. The onset at 385 nm was corresponded to a band gap of 3.23 eV.

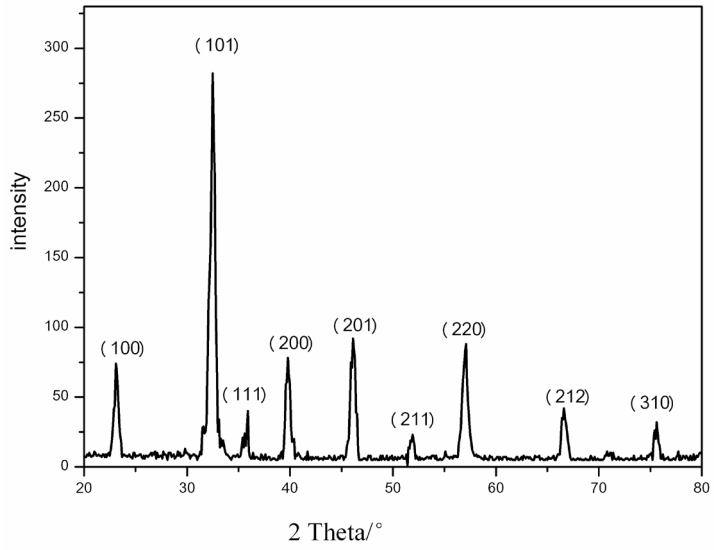

Figure 1. XRD pattern of $BaTiO_3$ film.

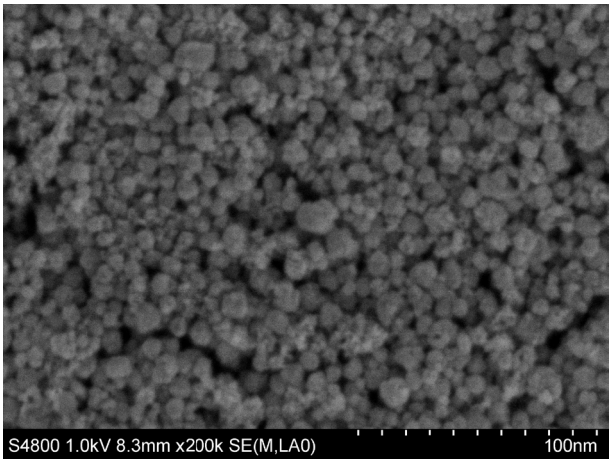

Figure 2. SEM image of $BaTiO_3$ film.

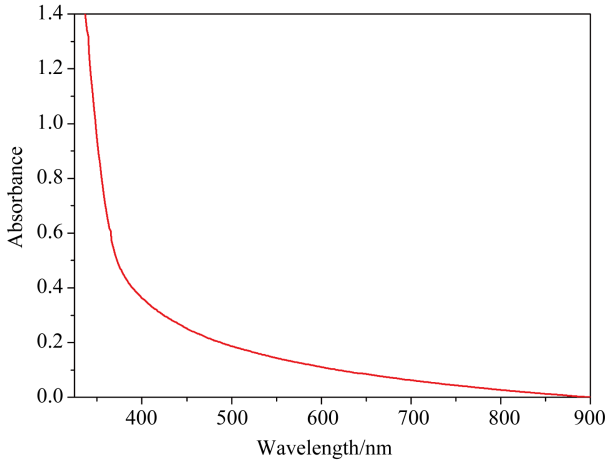

Figure 3. Absorption spectrum of a nanostructured $BaTiO_3$ film.

3.2. Spectroelectrochemistry and Flat Band Determination

All electrochemical and spectroelectrochemical experiments were carried out in a typical three-electrode system, in which a nanostructured $BaTiO_3$ electrode, a platinum wire and a saturated Ag/AgCl electrode acted as working, counter and reference electrodes respectively. Spectroelectrochemistry measurements were undertaken according to the published literature [10]. A quartz cell with three electrodes and electrolyte was incorporated into the sample compartment of a Shimadzu UV-vis spectrophotometer and connected to a CHI 800 potentiostat. All aqueous electrolyte solutions were prepared based on $LiClO_4$ as supporting electrolyte and the pH value of the electrolyte solutions was adjusted by $HClO_4$ (for pH 3.0) or NaOH (for pH 13.0). The electrolyte solutions were thoroughly degassed with N_2 prior to experiments. All potentials were given with reference to the saturated Ag/AgCl electrode. The working area of $BaTiO_3$ electrodes were 3 cm^2.

The potential-dependent absorption spectra of nanostructured $BaTiO_3$ electrodes measured in aqueous electrolytes of different pHs were shown in **Figure 4**. The absorbance increased at longer wavelengths as the application of more negative potential. The absorption onset shifted to more negative potential as pH increased.

Spectroelectrochemical measurement was usually applied for the monitoring of the electron filling in conduction band. Because the filling of electrons in conduction band could be monitored by the absorbance changes at long wavelength, the conduction band edge of a semiconductor could be calculated [11]-[13]. In **Figure 4**, the absorbance at 800 nm were plotted against applied potentials and shown in insetting figures. The flat band edges were closely dependent on pH of the electrolyte. The flat band edges were −0.70, −0.92 and −1.20 V at pH value of 3.0, 6.8 and 13.0 respectively.

The flat band potential is dependent on pH of electrolyte and is shown by the equations [10] [24]

$$E_{fb} = -\left(E_f^0/q\right) + \Delta E_H \tag{1}$$

$$\Delta E_H = 0.0592\left(pH_{PZC} - pH\right) \tag{2}$$

where pH_{PZC} is the pH at point of zero charge (PZC), E_f^0 is the Fermi level at pH_{PZC}, ΔE_H is the potential drop in Helmholtz layer. When pH is smaller than pH_{PZC}, there are net positive charges on surface, so $\Delta E_H > 0$. The smaller the pH is, the larger the ΔE_H is and the flat band potential shifts more positively. On the other hand, when pH is larger than pH_{PZC}, there are net negative charges on surface, so $\Delta E_H < 0$. The larger the pH is, the smaller the ΔE_H is and the flat band potential shifts more negatively.

The dependence of the flat band edge of a nanostructured $BaTiO_3$ film on pH of electrolyte is shown in **Figure 5**. A linear relation is obtained from fitting data linearly and expressed as $E_{fb} = -0.56 - 0.029$ pH.

3.3. Time-Resolved Current and Trap State Distribution

Time-resolved current at pH 3.0: The current-time curves of a nanostructured $BaTiO_3$ electrode were measured in $LiClO_4$ solution with the concentration of 0.2 $mol \cdot L^{-1}$ at the pH value of 3.0 under different potentials and were shown in **Figure 6(a)**. The applied potential was significantly influenced by the current. The currents were almost decreased to zero quickly when the potential was from 0 to −0.3 V. After the applied potential was more negative than −0.3 V, the current was decreased slowly. The results showed the band gap region was filled by trap. A nanostructured $BaTiO_3$ electrode had a flat band edge of −0.70 V at pH 3.0 (seen from **Figure 5**). When the potentials was more positive than −0.3 V, the density of traps was low, and thus the trap-filling time was short. At the same time, the decay of the time resolved current was fast [22]. On the other hand trap density was increased and the time of filling these traps needed long. The longest trap-filling time was −0.36 V which was just below the conduction band edge.

The accumulated charge Q under the current-time curves in **Figure 6(a)** was calculated and was shown in **Figure 6(b)**. If the accumulated charge Q from trap-filling reflects the density of states, Equation (3) can be obtained [12] [20]

$$N_{trap}(U) = (1/q)(dQ/dU) \tag{3}$$

where Q is accumulated charge, $N_{trap}(U)$ is density of trap states at potential U and q was electron charge. Equation (3) clearly indicates that trap density is directly proportional to dQ/dU, which provides a direct measurement of trap distribution. By differentiating the accumulated charge to the applied potential, a plot of dQ/dU against U is obtained and shown in the insert of **Figure 6(b)**. The totally trap states are 3.73×10^{15} cm^{-2}.

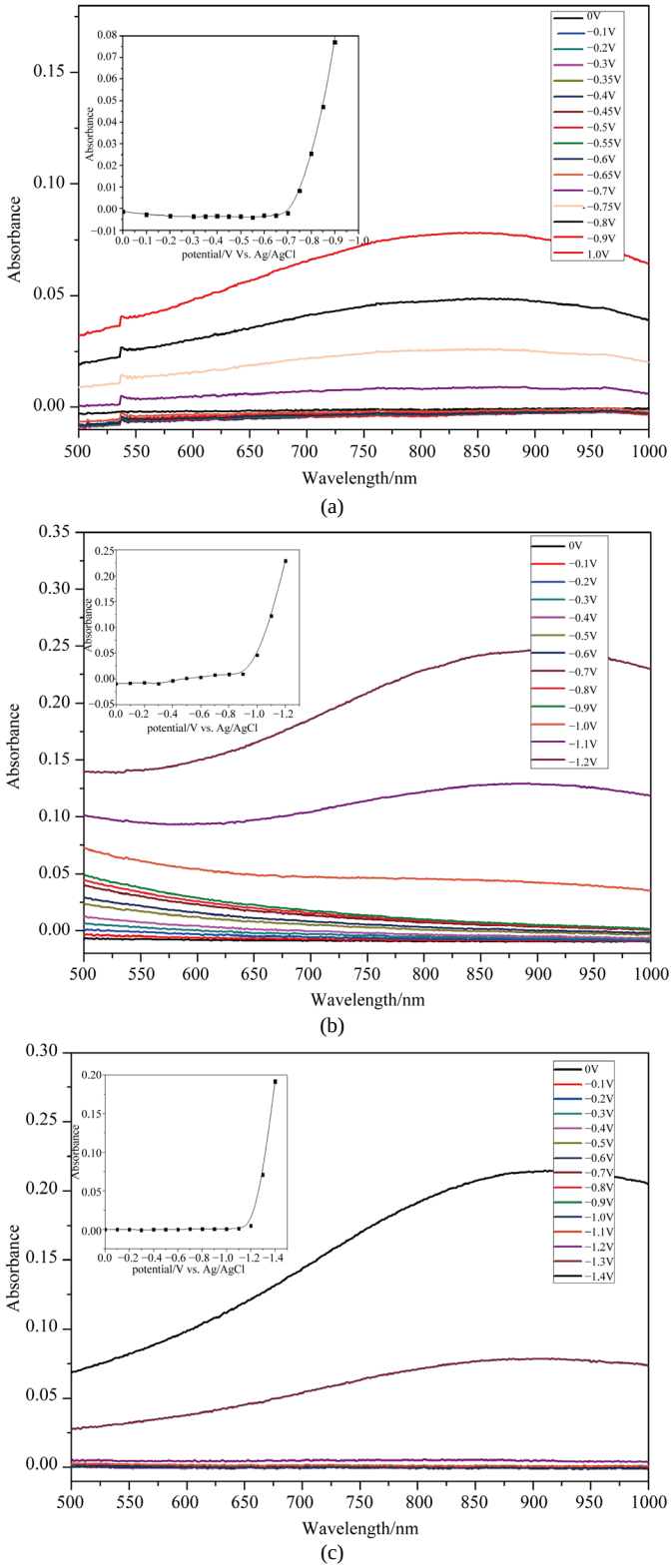

Figure 4. Differential spectra of nanostructured $BaTiO_3$ electrodes in: (a) 0.2 mol·L^{-1} $LiClO_4$ at pH 3.0; (b) 0.2 mol·L^{-1} $LiClO_4$ at pH 6.8; (c) 0.2 mol·L^{-1} $LiClO_4$ at pH 13.0. The inserts show absorbance changes at 800 nm. Spectra are recorded after polarized for 5 min at indicated potentials. The spectrum measured after stabilization for 15 min at +0.8 V has been subtracted.

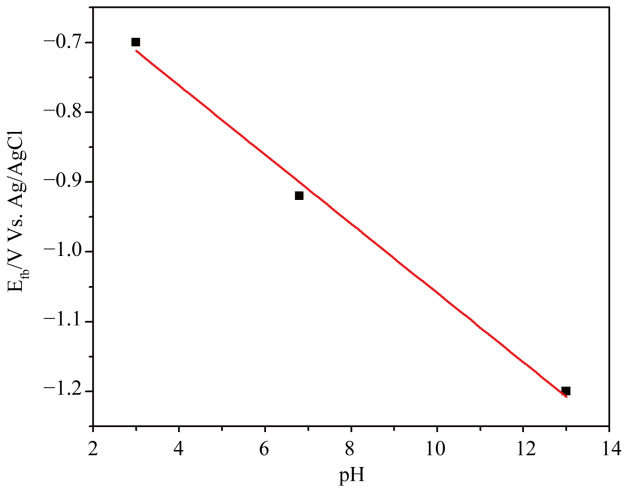

Figure 5. Flat band potential of nanostructured $BaTiO_3$ films as a function of pH.

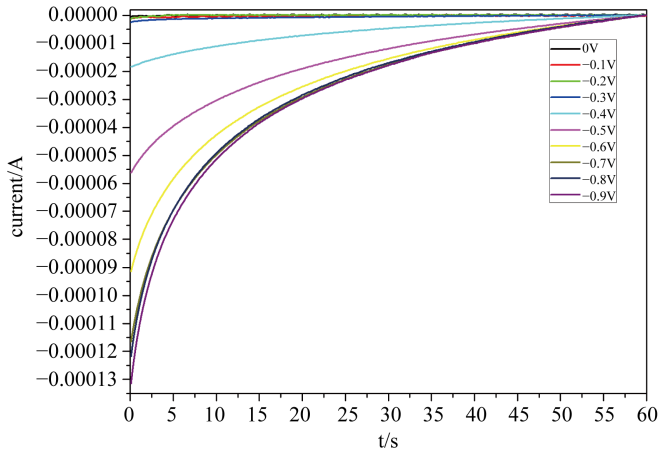

(a)

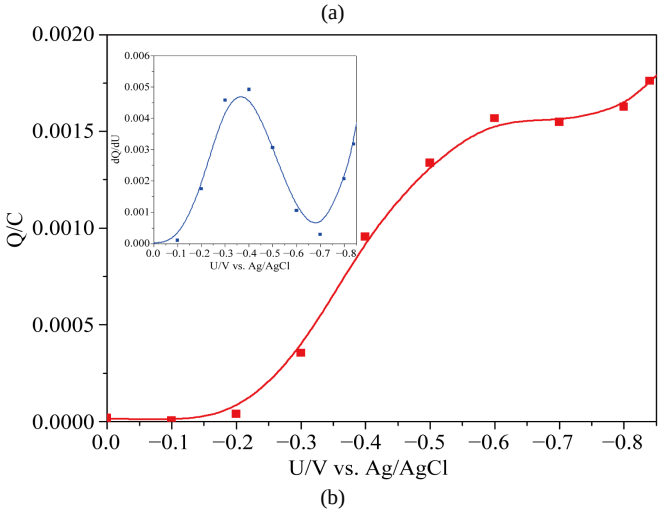

(b)

Figure 6. (a) Current-time curves of a nanostructured $BaTiO_3$ electrode in 0.2 mol·L^{-1} $LiClO_4$ of pH 3.0. The electrode was initially polarized at 0.8 V for 5 min and then measured at different applied potential. (b) Cathodic charges at different potentials derived by integrating the current-time curves in **Figure 6(a)**. The insert shows dQ/dU distribution against potential.

Time resolved currents at pH 6.8 and 13.0: The current-time curves in pH 6.8 and 13.0 solutions are similar to that in pH 3.0 solution and the cathodic charges at different potentials by integrating current-time curves measured in both solutions are shown in **Figure 7(a)**, **Figure 7(b)** and **Figure 8(a)**, **Figure 8(b)** respectively. The longest trap-filling time was at −0.5 V for pH 6.8 and −0.8 V for pH 13.0. The total amounts of trapped electrons were 4.02×10^{15} cm^{-2} for pH 6.8 and 6.48×10^{15} cm^{-2} for pH 13.0. It is obvious that the trap-filling process is faster in the pH 3.0 solution and pH 6.8 than that in pH 13.0 solution.

3.4. Cyclic Voltammetry and Surface Traps Determination

Cyclic voltammetry is a method for detecting and characterizing surface traps in nanocrystalline electrodes. A

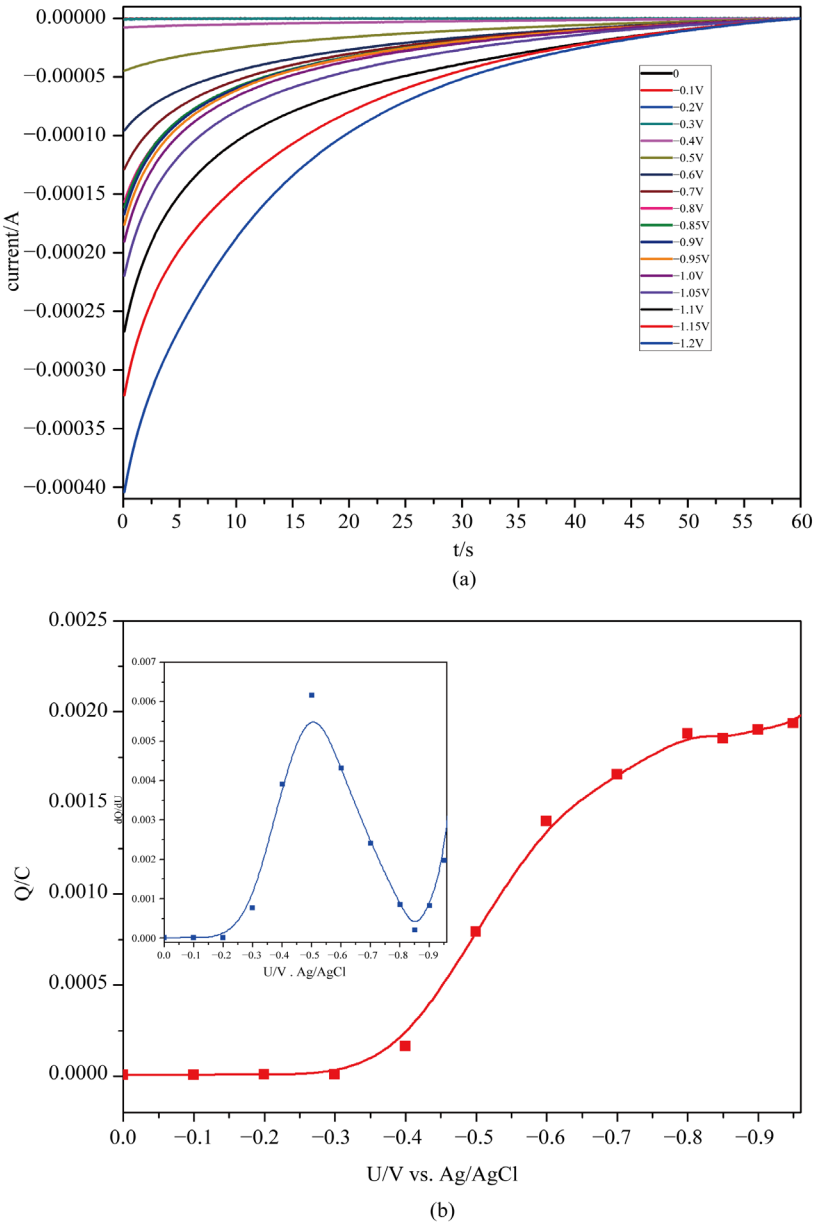

Figure 7. (a) Current-time curves of a nanostructured $BaTiO_3$ electrode in 0.2 $mol \cdot L^{-1}$ $LiClO_4$ of pH 6.8; (b) Cathodic charges accumulated at different potentials as derived by integrating the current-time curves at: pH 6.8. The insert shows dQ/dU distribution against potential.

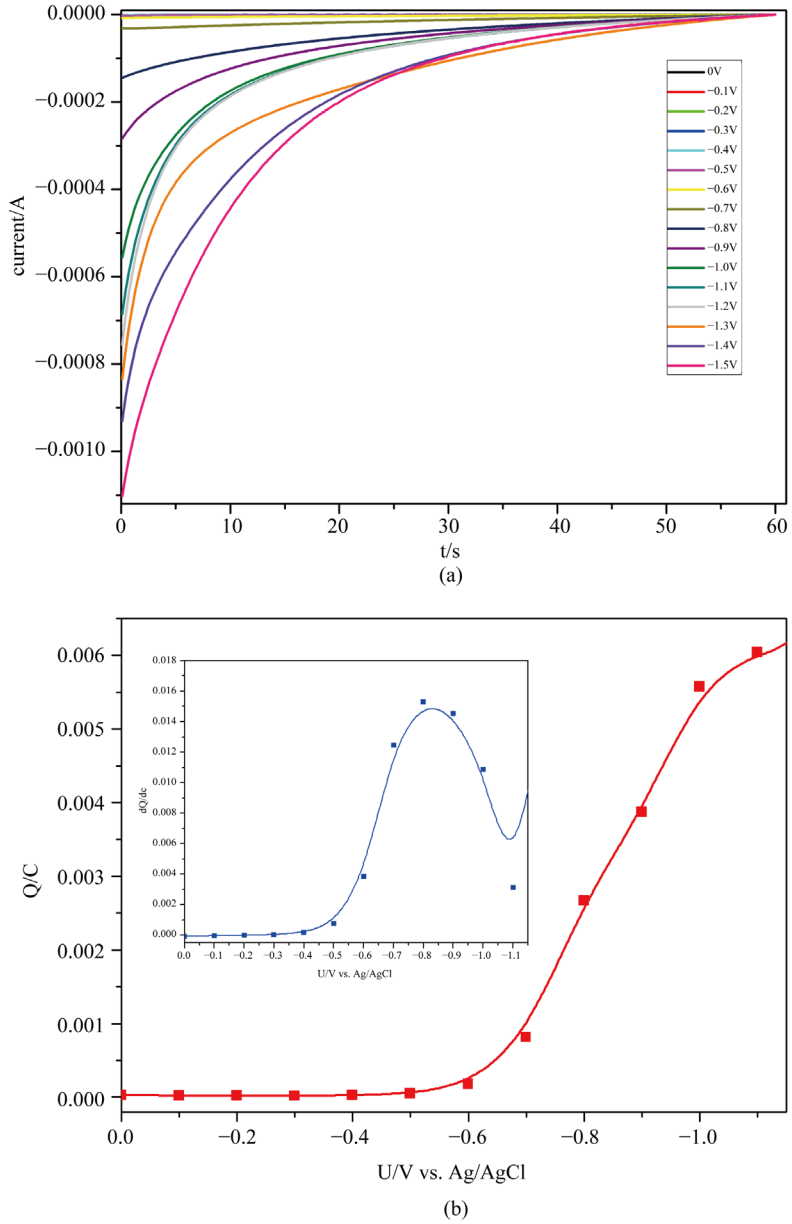

Figure 8. (a) Current-time curves of a nanostructured $BaTiO_3$ electrode in 0.2 mol·L^{-1} $LiClO_4$ of pH 13.0; (b) Cathodic charges accumulated at different potentials as derived by integrating the current-time curves at: pH 6.8. The insert shows dQ/dU distribution against potential.

shoulder was appeared in the current-potential curves which was more positive than the conduction band edge. The shoulder has been generally assigned to the presence of electron traps [12] [20]. The cyclic voltammograms of nanostructured $BaTiO_3$ electrodes were recorded at different pH and were shown in **Figure 9**.

The conduction-band edge of the nanostructured $BaTiO_3$ electrode at pH 3.0 is approximately at −0.70 V (see **Figure 5**) and a feature at −0.36 V in the cyclic voltammogram is corresponded to trap state filling below the conduction band edge which confirms the presence of surface traps [12] [25] [26]. The most trap state distribution at each pH are located at −0.36, −0.51, and −0.82 V at pH 3.0, 6.8, and 13.0 respectively, which are in good agreement with the results obtained from **Figure 6(b)**, **Figure 7(b)** and **Figure 8(b)**. It should be noticed that the size of the peak increases dramatically with pH increasing, so this well indicates that the traps are the most surface- related.

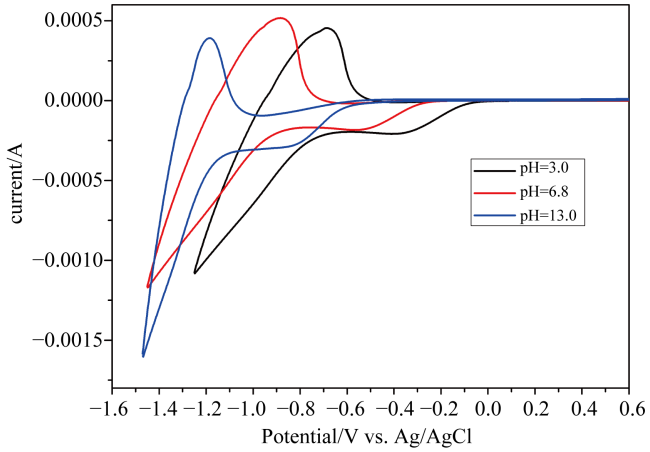

Figure 9. Cyclic voltammograms of nanostructured $BaTiO_3$ electrodes measured at different pH values. The electrodes were initially polarized at 0.8 V for 15 min before scanning, the scan rate was 5 mV/s.

4. Conclusion

Transparent nanostructured $BaTiO_3$ film electrodes have been synthesized and the band energetics and the flat band edges (E_{fb}) of nanostructured $BaTiO_3$ electrodes have been determined by electrochemical and spectroelectrochemical methods. The flat band edges of the nanostructured $BaTiO_3$ electrodes greatly depended on pH of electrolytes. The potentials turned more negative with the increase of pH value. The trap state distribution was investigated by the measurements of time resolved current. Total trap state densities were 3.73×10^{15}, 4.02×10^{15} and 6.48×10^{16} cm^{-2} at pH 3.0, 6.8 and 13.0 respectively with maximum located at −0.36 V, −0.50 V and −0.80 V. The CVs results were in good agreement with that obtained from the measurements of time-resolved currents. The size of the peak in the cyclic voltammograms increased dramatically with the increase in pH value, indicating that traps were the most surface-related.

Acknowledgements

This work was supported financially by the National Natural Science Foundation of China (Grant No. 20773103), Science & Technology Program of Education Department of Henan (12A150021).

References

[1] O'Regan, B. and Gratzel, M. (1991) A Low-Cost, High-Efficiency Solar Cell Based on Dye-Sensitized Colloidal TiO_2 Films. *Nature*, **353**, 3737-3740. http://dx.doi.org/10.1038/353737a0

[2] Murayama, M. and Mori, T. (2008) Novel Tandem Cell Structure of Dye-Sensitized Solar Cell for Improvement in Photocurrent. *Thin Solid Films*, **516**, 2716-2722. http://dx.doi.org/10.1016/j.tsf.2007.04.076

[3] Liu, J., Yang, H.T., Zhou, X.W. and Lin, Y. (2011) Photovoltaic Performance Improvement of Dye-Sensitized Solar Cells Based on Tantalum-Doped TiO_2 Thin Films. *Electrochimica Acta*, **56**, 396-400. http://dx.doi.org/10.1016/j.electacta.2010.08.063

[4] Hauch, A. and Georg, A. (2001) Diffusion in the Electrolyte and Charge-Transfer Reaction at the Platinum Electrode in Dye-Sensitized Solar Cells. *Electrochimica Acta*, **46**, 3457-3466. http://dx.doi.org/10.1016/S0013-4686(01)00540-0

[5] Gratzel, M. (2005) Solar Energy Conversion by Dye-Sensitized Photovoltaic Cells. *Inorganic Chemistry*, **44**, 6841-6851. http://dx.doi.org/10.1021/ic0508371

[6] van de Lagemaat, J., Park, N.G., Frank, A.J., Boschloo, G.K. and Goossens, A.J. (2000) Influence of Electrical Potential Distribution, Charge Transport, and Recombination on the Photopotential and Photocurrent Conversion Efficiency of Dye-Sensitized Nanocrystalline TiO_2 Solar Cells: A Study by Electrical Impedance and Optical Modulation Techniques. *The Journal of Physical Chemistry B*, **104**, 2044-2052. http://dx.doi.org/10.1021/jp993172v

[7] Cinnsealach, R., Boschloo, G., Rao, S.N. and Fitzmaurice, D. (1999) Coloured Electrochromic Windows Based on Nanostructured TiO_2 Films Modified by Adsorbed Redox Chromophores. *Solar Energy Materials and Solar Cells*, **57**, 107-125.

http://dx.doi.org/10.1016/S0927-0248(98)00156-1

[8] Razykov, T.M., Ferekides, C.S., Morel, D., Stefanakos, E., Ullal, H.S. and Upadhyaya, H.M. (2011) Solar Photovoltaic Electricity: Current Status and Future Prospects. *Solar Energy*, **85**, 1580-1608. http://dx.doi.org/10.1016/j.solener.2010.12.002

[9] Beermann, N., Boschloo, G., Holmberg, A. and Hagfeldt, A.J. (2002) Trapping of Electrons in Nanostructured TiO_2 Studied by Photocurrent Transients. *Journal of Photochemistry and Photobiology A: Chemistry*, **152**, 213-218. http://dx.doi.org/10.1016/S1010-6030(02)00236-8

[10] Enright, B. and Fitzmaurice, D. (1996) Spectroscopic Determination of Electron and Hole Effective Masses in a Nanocrystalline Semiconductor Film. *The Journal of Physical Chemistry*, **100**, 1027-1035. http://dx.doi.org/10.1021/jp951142w

[11] Fu, Z.W., Huang, F., Zhang, Y., Chu Y. and Qin, Q.Z. (2003) The Electrochemical Reaction of Zinc Oxide Thin Films with Lithium. *Journal of Electrochemical Society*, **150**, A714-A720. http://dx.doi.org/10.1149/1.1570410

[12] Yang, S.M., Kou, H.Z., Wang, H.J., Cheng K. and Wang, J.C. (2010) Preparation and Band Energetics of Transparent Nanostructured SrTiO3 Film Electrodes. *The Journal of Physical Chemistry C*, **114**, 815-819. http://dx.doi.org/10.1021/jp910204q

[13] O'Regan, B., Moser, J., Anderson M. and Gratzel, M. (1990) Vectorial Electron Injection into Transparent Semiconductor Membranes and Electric Field Effects on the Dynamics of Light-Induced Charge Separation. *The Journal of Physical Chemistry*, **94**, 8720-8726. http://dx.doi.org/10.1021/j100387a017

[14] Wang, H., Hagfeldt, A., Lindquist, S.E., Boschloo, G. and Lindstrom, H. (2001) Electrochemical Investigation of Traps in a Nanostructured TiO_2 Film. *The Journal of Physical Chemistry B*, **105**, 2529-2533. http://dx.doi.org/10.1021/jp0036083

[15] Ma, B., Bai J.C., and Dong , L.F. (2013) Electrochemical Impedance Analysis of Methanol Oxidation on Carbon Nanotube-Supported Pt and Pt-Ru Nanoparticles. *Journal of Solid State Electrochemistry*, **17**, 2783-2788. http://dx.doi.org/10.1007/s10008-013-2177-1

[16] Juodkazis, K., Juodkazyte, J., Sebeka, B., Savickaja, I. and Juodkazis, S. (2013) Photoelectrochemistry of Silicon in HF Solution. *Journal of Solid State Electrochemistry*, **17**, 2269-2276. http://dx.doi.org/10.1007/s10008-013-2064-9

[17] Juodkazis, K., Juodkazyte, J., Kalinauskas, P., Gertus, T., Jelmakas, E., Misawa, H. and Juodkazis, S. (2010) Influence of Laser Microfabrication on Silicon Electrochemical Behavior in HF Solution. *Journal of Solid State Electrochemistry*, **14**, 797-802. http://dx.doi.org/10.1007/s10008-009-0852-z

[18] Badawy, W.A. (2008) Effect of Porous Silicon Layer on the Performance of Si/Oxide Photovoltaic and Photoelectrochemical Cells. *Journal of Alloys and Compounds*, **464**, 347-351. http://dx.doi.org/10.1016/j.jallcom.2007.09.122

[19] da Silva, L.F., Maia, L.J.Q., Bernardi, M.I.B., Andres J.A. and Mastelaro, V.R. (2011) An Improved Method for Preparation of $SrTiO_3$ Nanoparticles. *Materials Chemistry and Physics*, **125**, 168-173. http://dx.doi.org/10.1016/j.matchemphys.2010.09.001

[20] Yang, S.M., Kou, H.Z., Wang, H.J. and Xue, H.B. (2010) Tunability of the Band Energetics of Nanostructured SrTiO3 Electrodes for Dye-Sensitized Solar Cells. *The Journal of Physical Chemistry C*, **114**, 4245-4249. http://dx.doi.org/10.1021/jp9117979

[21] Xu, J.B., Zhai, J.W., Yao, X., Xue, J.Q. and Huang, Z.M. (2007) Dielectric and Optical Properties of $BaTiO_3$ Thin Films Prepared by Low-Temperature Process. *Journal of Sol-Gel Science and Technology*, **42**, 209-212. http://link.springer.com/article/10.1007/s10971-007-0740-x

[22] Shen, Z.G., Zhang, W.W., Hen J.F. and Jimmy, Y. (2006) Low Temperature One Step Synthesis of Barium Titanate: Particle Formation Mechanism and Large-Scale Synthesis. *Chinese Journal of Chemical Engineering*, **14**, 642-648. http://dx.doi.org/10.1016/S1004-9541(06)60128-6

[23] Barbe, C.J., Arendse, F., Comte, P., Jirousek, M., Lenzmann, F., Shklover, V. and Gratzel, M. (1997) Nanocrystalline Titanium Oxide Electrodes for Photovoltaic Applications. *Journal of the American Ceramic Society*, **80**, 3157-3171. http://onlinelibrary.wiley.com/doi/10.1111/j.1151-2916.1997.tb03245.x/citedby

[24] Sikora, E., Sikora, J. and Macdonald, D.D. (1996) A New Method for Estimating the Diffusivities of Vacancies in Passive Films. *Electrochimica Acta*, **41**, 783-789. http://dx.doi.org/10.1016/0013-4686(95)00312-6

[25] Kavan, L., Kratochvilova, K., and Gratzel, M. (1995) Study of Nanocrystalline TiO2 (Anatase) Electrode in the Accumulation Regime. *Journal of Electroanalytical Chemistry*, **394**, 93-102. http://dx.doi.org/10.1016/0022-0728(95)03976-N

[26] Kavan, L., Gratzel, M., Rathousky, J. and Zukal, A. (1996) Nanocrystalline TiO_2 (Anatase) Electrodes: Surface Morphology, Adsorption, and Electrochemical Properties. *Journal of Electrochemical Society*, **143**, 394-400. http://dx.doi.org/10.1149/1.1836455